Materials and methods

Endothelial immunofluorescence in human carotid arteries.

Human atherosclerotic plaques obtained from 5 patients were remnants of the surgical specimen routinely processed for pathology following *en bloc* carotid endarterectomy surgery performed after patient consent. Institutional Review Board approval was not required for the specimens at the time the work was done. The surgeon identified the upstreaming from the downstream area of the lesion using a silk threat. The clinical features of these patients are presented in SI Appendix, Table S1. The plaques were immediately scraped off in order to isolate endothelial cells. The upstream part of the plaque was defined as the area between the beginning of the plaque and the site of maximal stenosis. The downstream part was defined as the area between the site of maximal stenosis and the end of the plaque. Endothelial cells coming from the upstream (high SS) or the downstream (low SS) part of the plaque were collected separately (1,2). Plaques were included in this study when upstream and downstream parts were clearly visible and occlusion was absent. We did not include plaques with erosion or rupture because we could not determine whether the rupture occurred *in vivo* or during the surgical manipulation of the specimen. Endothelial cells were then pulled down on a slide using a cytospin centrifuge (Cytospin™ 4 Cytocentrifuge, Thermo scientific), fixed in 4% paraformaldehyde and permabilized (0.01% triton-X100). Cells were incubated with an anti-LC3 antibody (SI Appendix, Table S2) and then with secondary antibody (anti-rabbit AlexaFluor594, Life technologies). Co-staining with anti-CD31 antibody (using a secondary anti-goat AlexaFluor488 antibody, Life technologies) was performed to identify endothelial cells. Cells were then co-stained with DAPI (0.1 µg/mL, Sigma) in order to identify cell nuclei. Samples were analyzed using a Zeiss Axio Imager Z1 fluorescence microscope equipped with a Zeiss ApoTome system (Zeiss).

Human Umbilical Vein Endothelial Cell culture.

Confluent Human Umbilical Vein Endothelial cells (HUVEC; passage 2 to 4; 10 different primary cultures were used; Promocell, Heidelberg, Germany) were cultured on 0.2 %

gelatin-coated slides (Menzel Glazer; Braunschweig, Germany) in endothelial cell basal medium containing growth factors, 1 % fetal calf serum (Promocell), streptomycin (100 IU/mL), penicillin (100 IU/mL) and Amphotericin B (10 μg/L) (Gibco).

Plasmid electroporation.

DNA vector encoding the tandem mRFP-GFP-LC3 was used to transiently express the RFP-GFP tagged LC3 protein, in order to monitor the LC3 translocation and autophagosomes fusion with lysosomes. In the absence of autophagy induction, the LC3 fluorescent signals are evenly distributed; upon autophagy induction, punctate fluorescent signals (yellow LC3 dots) appear as a result of LC3 accumulation on the membrane of autophagosomes; when fusion with lysosomes occurs, the punctate signal becomes red by acidic degradation of the GFP. Cells were used at 50 to 60% confluence for cDNA transfection by use of Nucleofector (Lonza/Amaxa) according to the manufacturer's instructions. Briefly, 5×10^6 HUVECs were electroporated with 2 μg of plasmid, using the U-01 program, and then replated in endothelial cell basal medium containing 1% fetal calf serum for 6h. The medium was then changed and cells reached confluence within 48 hours. Transfection efficacy was assessed by expression of fluorescent LC3 protein.

Lentiviral transduction.

Lentiviruses expressing inducible shRNA (Sigma Aldrich) were used to silence Kinesin-like protein (KIF3A), ATG5 and CD31. HUVECs were infected in the presence of hexadimethrine bromide (at 8 μg/mL) with lentiviruses at multiplicity of infection (MOI) 2.5 for KIF3a and ATG5 or MOI 5 for CD31. Negative controls were lentiviruses expressing a non-target shRNA used at the same MOI as for the protein of interest. Transduced cells were amplified and selected using puromycine (Sigma Aldrich #P9620) at 1 μg/mL during amplification and experiments. ShRNA expression was induced by treating HUVECs for 10 days using Isopropyl β-D-1-thiogalactopyranoside (IPTG, Sigma Aldrich; #I6758) at 1 mmol/L for KIF3A, 0.1 mmol/L for CD31 and 5 days at 1 mmol/L for ATG5.

Shear stress experiment in vitro.

A unidirectional steady laminar SS was applied to confluent HUVECs using a parallel plate chamber system as described elsewhere (3). Endothelial cell medium previously filtered on a 0.1 μm membrane was perfused at different rates and for different times (1 min to 48 hours). Local SS was calculated using Poiseuille's law and was 20, 2 or 0 dynes/cm^2, corresponding to high, low SS or static conditions, respectively.

In some experiments, cells were treated with Bafilomycin A1 (Vacuolar-type H+ -ATPase inhibitor, 100 nmol/L) for 2 hours before ending the SS experiment in order to assess autophagic flux, or with rapamycin (0.5 µmol/L, Sigma) or wortmannin (5 µmol/L, Sigma) in order to modulate autophagy level. For inflammation experiments, cells were treated with TNFα (1 ng/mL) 12 hours before the end of the flow experiment. In control conditions, HUVECs were incubated with the same concentration of the solvent (DMSO). Cells were then collected for Western blot, immunofluorescent microscopy or transmission electron microscopy, as detailed below. For ELISA, the supernatant were collected after the SS experiment, centrifuged for 15 minutes at 600g in order to remove cell debris and stored at -80°C until analysis.

Immunofluorescent staining and Immunofluorescence microscopy in vitro.

After SS exposure, HUVECs were fixed with 4% PFA and permeabilized using 0.1% Triton X-100 and blocked with 5% bovine serum albumin for 1 hour. To assess autophagy flux, cells were incubated with an anti-LC3 antibody and an anti-LAMP2 antibody (SI Appendix, Table S2) and then with secondary antibody (anti-rabbit AlexaFluor594 or anti-goat AlexaFuor 488 respectively, Life technologies). Autophagic flux was also assessed using cells transfected with the tandem mRFP-GFP-LC3 plasmid and exposed to SS. Images were acquired using a Leica SP5 confocal microscope (Leica).

For assessment of the morphology and orientation of endothelial cells under shear stress, HUVECs were stained with an anti-CD144 antibody (SI Appendix, Table S2) and a

secondary anti-goat AlexaFluor594 antibody (Life technologies). Samples were analyzed using a Zeiss Axio Imager Z1 fluorescence microscope equipped with a Zeiss ApoTome system (Zeiss).

For all the immunofluorescence experiments, samples were costained with DAPI (0.1 µg/mL, Sigma) in order to identify cell nuclei.

Transmission electron microscopy (TEM).

Transmission electron microscopy observations were performed at the IFR83-Jussieu-Paris core facility. Briefly, HUVECs were fixed with Karnovsky's fixative adapted for vascular tissues and cells (2% paraformaldehyde, 2.5% glutaraldehyde and 0.1 mol/L sodium phosphate buffer, Electron Microscopy Sciences, Hatfield, PA). After dehydration in ethanol, cells were embedded in Epon. Grids were analyzed with a transmission electron microscope (EM 912 OMEGA, ZEISS) equipped with a LaB6 filament at 80 kV. Images were captured with a digital camera (SS-CCD, Proscan 1kx1k) and with custom software.

For morphometric analysis, a minimum of 10 random fields per condition and per experiment were taken in a blinded manner at a magnification of 23,200x (>450 µm² per condition and per experiment). Electron microscopy findings were then assessed by 3 readers (ACV, PER and AH) unaware of SS condition. For TEM experiments, the term autophagic vesicle refers to autophagosome or autolysosome since it is often not possible to determine from TEM images whether or not an autophagosome has fused with a lysosome (4).

In vitro LC3 assessment using flow cytometry.

After exposure to SS, HUVECs were permeabilized using 0.2% saponin for 10 minutes and then washed 3 times with phosphate buffered saline (PBS). Saponin specifically extracts the nonautophagosome-associated form of LC3 (5). Then, HUVECs were fixed in 95% ethanol and incubated with an anti-LC3 antibody (SI Appendix, Table S2) and with an anti-rabbit anti-rabbit AlexaFluor488 antibody as described (5). Costaining with propidium iodide for 5 min prior to flow cytometry analysis was performed to identify live cells and exclude cell

aggregates. HUVECs were analyzed using a LSRII flow cytometer (BD Biosciences), and results were expressed as mean fluorescent intensity among live cells.

Senescence-associated beta-galactosidase activity in vitro.

SA-β-galactosidase activity was assessed by flow cytometry using a fluorogenic substrate (C_{12}FDG, Invitrogen). After exposure to SS, HUVECs were pretreated with chloroquine (300 µmol/L, Sigma) diluted in endothelial cell medium without phenol red for 1 hr in order to increase the internal pH of lysosomes to 6. C_{12}FDG (33 µmol/L) was then added to the medium for 1 hr. HUVECs were then washed with PBS at 4°C, resuspended and analyzed immediately using a LSR FortessaTM flow cytometer (BD Biosciences). Light scatter parameters were used to exclude dead cells and subcellular debris. The C_{12}-fluorescein signal was acquired using the FL1 detector. Data were analyzed using FlowJo software to determine the percentage of SA-β-gal positive cells. Cells not treated with C_{12}FDG were used as a negative control.

Animal models.

All mice were on a C57BL/6 background with the exception of *Ampkα1 -/-* mice, which were on a mixed C57Bl6/129 Sv background due to embryonic letality on C57Bl6 background.

Mice constitutively deficient in endothelial autophagy were obtained by crossing *VE-cadherin-Cre* transgenic mice provided by M. Souyri (6), with *Atg5*$^{flox/flox}$ mice provided by N. Mizushima (7) or *Atg7*$^{flox/flox}$ mice were provided by M. Komatsu (8). For characterization of baseline morphological and metabolic features and assessment of endothelial apoptosis, mice were fed a chow diet and were euthanized between 8 and 17 weeks of age. For assessment of endothelial p53 expression, 13 to 17 week old mice were fed a high fat diet (D12492, 26.2% protein, 26.3% carbohydrate, 34.9% fat weight to weight, Research Diets) for 5 weeks and were euthanized (9). For assessment of endothelial senescence, 42 to 54 week old mice were fed the same high fat diet for 16 weeks and were euthanized (10).

To investigate the effect of endothelial autophagy on atherosclerosis development, mice constitutively deficient in endothelial autophagy (*Atg5$^{flox/flox}$;VE-cadherin-Cre*) were crossed with *ApoE$^{-/-}$* mice purchased from the Charles Rivers laboratory. 13 week-old mice were fed a western diet (D12079B, 20% protein, 50% carbohydrate, 21% fat weight to weight, Research Diets) for 10 weeks and were then euthanized. AMPKα*1-/-* mice were described previously (11). *CD31-/-* mice were provided by T.W. Mak (12). All experiments were performed in accordance with the European Community guidelines for the care and use of laboratory animals (N°07430) and were approved by our institutional ethical committee (02526.02).

For investigation of autophagic flux *in vivo*, 8 to 9 weeks old C57BL/6 mice were injected intraperitoneally with chloroquine (60 mg/kg/day for 3 consecutive days, as described previously (13)) or rapamycin (4 mg/kg/day for 2 consecutive days) or with the corresponding vehicle.

Blood pressure measurement.

Arterial blood pressure was measured every 30 seconds at the tail of conscious mice using a CODA non-invasive blood pressure device (Kent Scientific Corporation) (mean value of 15 measurements). Blood pressure was measured for 3 consecutive days after 2 days of acclimation in the chamber.

Fasting plasma glucose and cholesterol levels.

Three days before sacrifice, mice were fasted for 6 hours. For blood glucose analysis, the distal 1 mm of the tail was excised using sterile scissors. The first blood drop was discarded; then serum glucose level was determined using OneTouch Ultra® reactive strips and OneTouch Ultra® reader (Lifescan). For plasma cholesterol analysis, mice were anesthetized with 2% isoflurane. Then, 75 μL of blood were collected from the peri-orbital venous sinus using a heparinized microhematocrit tube (Hirschmann-Laborgeräte). Blood was then centrifuged twice at 2,500 g for 15 min at room temperature to prepare platelet free

plasma and stored at -80°C until analysis. Plasma cholesterol level was determined using the Cholesterol RTU™ commercial kit (BioMérieux).

Plasma preparation.

On the day of sacrifice, non-fasted mice were sedated with 2% isofluorane. Blood was collected from the inferior vena cava using a 25 gauge x 1' needle in a 1 mL syringe pre-coated with 3.8% sodium citrate. The mice were then humanely euthanized. Blood was centrifuged at 1,500 g for 15 minutes at 18°C in order to pellet cells. Then, plasma was centrifuged at 13,000 g for 5 minutes at 18°C to pellet platelets and cell debris. Platelet free plasma (PFP) was aliquoted and stored at -80°C for measurement of circulating levels of inflammatory molecules.

Senescence-associated beta-galactosidase assay on mouse aortas.

Mouse aortas were collected fresh, micro-dissected under a Nikon SMZ 745 dissecting microscope to remove extra fat and fixed for 8 min in 2% formaldehyde and 0.2% glutaraldehyde in PBS. Beta-galactosidase staining was performed by incubating the aortas for 48 hours at 37°C in a CO_2-free incubator with a fresh staining solution containing 1 mg/mL X-gal, 0.2 mol/L citric acid/sodium phosphate, 5 mmol/L potassium ferrocyanide, 5 mmol/L potassium ferricyanide, 150 mmol/L NaCl and 2 mmol/L $MgCl_2$ at pH 6.0. After staining, aortas were washed with PBS, mounted "*en face*" on glass slides and imaged using a bright field Zeiss Axio Imager Z1 (Zeiss) microscope. Images were acquired at 100 X magnification and the number of SA-β-gal positive cells/μm^2 was quantified by two independent operators (MK and JP) unaware of mice genotype.

Red-oil staining.

Mouse aortas were first injected with PBS then with PBS supplemented with 4% paraformaldehyde, dissected and kept in PBS supplemented with 4% paraformaldehyde for 2 hours. Then, aortas were stained with a freshly prepared Oil Red O working solution (40%

distilled water, 60% of a 5 g/L Oil Red O in isopropanol; Sigma) for 30 minutes under agitation. Aortas were then differentiated using 70% ethanol for 5 minutes, mounted "*en face*" on glass slides and then observed using a bright field microscope (Leica M165FC, camera 425). Plaque size was quantified using the ImageJ software.

Murine aortic endothelial cell isolation.

The mouse vasculature was rinsed by injecting *in situ* 10 mL of Dulbecco's modified Eagle's medium (DMEM) (Gibco) into the left ventricle. Aortas were then retrieved, injected with 1 mg/mL type II Collagenase (Worthington) using a BD Insyte™ Autoguard™ catheter (BD) and incubated at 37°C for 45 minutes. Mouse aortic endothelial cells (MAEC) were collected by flushing the aortas with 10 mL DMEM, and then pelleted by centrifugation at 1000 g for 7 min before being seeded in a 0.1% gelatin-coated 12 well plate in DMEM supplemented with 20 % fetal calf serum (Gibco). After 24 hours, the medium was changed to Endothelial cell growth medium MV with growth factors (Promocell) and 5% fetal calf serum. By flow cytometry, we observed that 92% and 62% of the MAECs were positive for the endothelial markers CD-31 and eNOS, respectively and 0% were positive for smooth muscle cell and fibroblast markers (α-SMC-actin and ER-TR7, respectively). MAECs were used for Western blot analysis after one passage.

***En face* immunofluorescence microscopy on mouse aortas.**

Mouse aortas were injected *in situ* with PBS supplemented with 4% paraformaldehyde. After dissection, the tissues were permeabilized using 0.2% Triton X-100 and blocked with 5% bovine serum albumin for 20 minutes. To assess autophagy level, aortas were first incubated with an anti-LC3 antibody (SI Appendix, Table S2) and then with secondary antibody (anti-rabbit AlexaFluor594, Life technologies). To assess p53 and p16 localization, aortas were first incubated with an anti-p53 or an anti-p16 antibody (SI Appendix, Table S2) and then with secondary antibody (anti-mouse AlexaFluor594, Thermo Scientific, respectively). To assess apoptosis level, aortas were stained with the *in situ* cell death detection kit from Roche (red,

Neuilly-sur-Seine, France) according to manufacturer's instructions. In all experiments, endothelial cells were easily recognized by their morphology. Still, in most series of experiment, a co-staining with anti-CD31 antibody (using a secondary anti-goat AlexaFluor488 antibody, Life technologies) or anti-CD144 antibody (Santa Cruz biotechnology sc-6458) was performed. In all mice, 8 to 10 images were obtained from regions in the aortic arch exposed to low SS and the thoracic aorta exposed to high SS. For all these immunofluorescence experiments samples were co-stained with DAPI (0.1 µg/mL, Sigma) in order to identify cell nuclei. Samples were analyzed using a Zeiss Axio Imager Z1 fluorescence microscope equipped with a Zeiss ApoTome system (Zeiss).

ELISA.

Levels of MCP-1 in surpernatant of HUVECs were assessed by an ELISA assay (R&D, human MCP-1 Duo-set DY279) following the manufacturer's instructions.

Immunoblotting.

HUVECs or MAECs were washed with cold PBS and scraped off in RIPA buffer (150 mmol/L NaCl, 50 mmol/L TrisHCl, pH 7.4, 2 mmol/L EDTA, 0.5% sodium deoxycholate, 0.2% sodium dodecyl sulfate, 2 mmol/L activated orthovanadate, complete protease inhibitor cocktail tablet (Complet mini, Roche, France) and complete phosphatase inhibitor cocktail tablet (Roche, France)). Lysates were sonicated (15 seconds, 40 watts, Vibra Cell, Bioblock), and protein content was quantified using the Lowry protein assay (Bio-Rad; Hercules, CA). Lysates were mixed with the reducing sample buffer for electrophoresis and subsequently transferred onto nitrocellulose (Bio-Rad) for all blots except for p16, KLF-2, p-ACC and ACC (PVDF membranes, Thermo Scientific). Equal loading was checked using Ponceau red solution. Membranes were incubated with primary antibodies (SI Appendix, Table S2). After secondary antibody incubation (anti-goat, anti-rabbit, anti-rat or anti-mouse, Amersham, GE Healthcare, UK 1/3000), immunodetection was performed using an enhanced chemiluminescence kit (Immun-Star Western C kit, Bio-Rad, or WesternBright™ Sirius,

Advansta for p16 blot) and bands were revealed using the Las-4000 imaging system. After initial immunodetection, membranes were stripped of antibodies and re-probed with anti-GAPDH, anti-actin or anti anti-tubulin antibodies (SI Appendix, Table S2). Values reported from Western blots were obtained by band density analysis using Image Gauge software (Fujifilm, Tokyo, Japan) and expressed as the ratio protein of interest compared to GAPDH, actin or tubulin expression for whole cell extract.

Statistical analysis.

Data are expressed as mean ± SEM for *in vitro* experiments and as median (interquartile range) for *in vivo* experiments. Comparisons between different SS conditions or between control and treatment conditions were performed using a Wilcoxon test. Comparisons between groups of mice were performed using the Mann-Whitney U-test. Comparison between genders was performed using a Chi-square test. Statistical analyses and Figures were performed using the SPSS statistical package 20.0 software for Windows (SPSS Inc., Chicago, IL, United States) and GraphPad Prism 5 software, respectively. All tests were two-sided and used a significance level of 0.05.

Data sharing.

The data that support the findings of this study are available from the corresponding author on reasonable request.

References :

1. Tricot O*, et al.* (2000) Relation between endothelial cell apoptosis and blood flow direction in human atherosclerotic plaques. *Circulation* 101(21):2450-2453.

2. Choi G*, et al.* (2015) Coronary Artery Axial Plaque Stress and its Relationship With Lesion Geometry: Application of Computational Fluid Dynamics to Coronary CT Angiography. (Translated from eng) *JACC Cardiovasc Imaging* 8(10):1156-1166 (in eng).
3. Ramkhelawon B*, et al.* (2009) Shear stress regulates angiotensin type 1 receptor expression in endothelial cells. *Circ Res* 105(9):869-875.

4. Eskelinen EL (2005) Maturation of autophagic vacuoles in Mammalian cells. *Autophagy* 1(1):1-10.

5. Eng KE, Panas MD, Karlsson Hedestam GB, & McInerney GM (2010) A novel quantitative flow cytometry-based assay for autophagy. *Autophagy* 6(5):634-641.

6. Oberlin E*, et al.* (2010) VE-cadherin expression allows identification of a new class of hematopoietic stem cells within human embryonic liver. *Blood* 116(22):4444-4455.
7. Hara T*, et al.* (2006) Suppression of basal autophagy in neural cells causes neurodegenerative disease in mice. *Nature* 441(7095):885-889.
8. Komatsu M*, et al.* (2005) Impairment of starvation-induced and constitutive autophagy in Atg7-deficient mice. *J Cell Biol* 169(3):425-434
9. Warboys CM*, et al.* (2014) Disturbed flow promotes endothelial senescence via a p53-dependent pathway. (Translated from eng) *Arterioscler Thromb Vasc Biol* 34(5):985-995 (in eng).
10. Wang CY*, et al.* (2009) Obesity increases vascular senescence and susceptibility to ischemic injury through chronic activation of Akt and mTOR. *Sci Signal* 2(62):ra11.
11. Jorgensen SB*, et al.* (2004) Knockout of the alpha2 but not alpha1 5'-AMP-activated protein kinase isoform abolishes 5-aminoimidazole-4-carboxamide-1-beta-4-ribofuranosidebut not contraction-induced glucose uptake in skeletal muscle. (Translated from eng) *J Biol Chem* 279(2):1070-1079 (in eng).
12. Duncan GS*, et al.* (1999) Genetic evidence for functional redundancy of Platelet/Endothelial cell adhesion molecule-1 (PECAM-1): CD31-deficient mice reveal PECAM-1-dependent and PECAM-1-independent functions. *J Immunol* 162(5):3022-3030.
13. Orhon I*, et al.* (2016) Primary-cilium-dependent autophagy controls epithelial cell volume in response to fluid flow. (Translated from eng) *Nat Cell Biol* 18(6):657-667 (in eng).

Age (yrs)	79 (72-85)
Male gender	4 (80)
Symptomatic plaques	2 (40)
Stroke	1 (20)
Amourosis	1 (20)
Cardio-vascular risk factors	
Diabetes	2 (40)
Hypertension	3 (60)
Smoking	1 (20)
Dyslipidemia	4 (80)
Body mass index (kg/m²)	28.7 (21.9-35.3)
Treatments	
Antiplatelet therapy	5 (100)
Statins	4 (80)
Beta-blockers	2 (40)
Angiotensin-converting enzyme inhibitors or Angiotensin II receptor antagonist	3 (60)
Calcium channel blockers	1 (20)
Diuretics	2 (40)

Table S1. Patient's characteristics. Data are expressed as median (interquartile range) or frequency (%) (n = 5).

Antibody anti-	Raised in	Reference		Dilution	WB Buffer	IF buffer
4EBP1	rabbit	CST	9452	1/1000	TBST milk	-
phospho-4EBP1 (Thr37/46)	rabbit	CST	2855	1/1000	TBST BSA	-
AMPK	rabbit	CST	2795	1/1000	TBST milk	-
phospho-AMPK (Thr172)	rabbit	CST	2535	1/1000	TBST BSA	-
ATG5	rabbit	CST	8540	1/500	TBST milk	-
ATG7	rabbit	CST	2631	1/1000	TBST milk	-
BECLIN1	rabbit	CST	3495	1/1000	TBST milk	-
CD144	goat	Santa Cruz	sc-6458	1/100	-	PBS BSA
CD31	goat	Santa Cruz	sc-1506	1/200	TBST milk	PBS BSA
CD41	rat	BD Pharmingen	563317	1/20		PBS BSA
ICAM1	goat	R&D	AF796	1/1000	TBST milk	-
KLF-2	goat	Novus biological	NB-10-1051	1/500	TBST milk	
KIF3a	rabbit	Abcam	ab11259	1/2000	TBST milk	-
ULK1	rabbit	CST	4773	1/1000	TBST milk	-
phospho-ULK1 (Ser555)	rabbit	CST	5869	1/1000	TBST BSA	-
LAMP2	goat	Santa Cruz	sc-8101	1/1000	TBST milk	PBS BSA
LC3B	rabbit	CST	2775	1/1000	TBST milk	PBS BSA
p16	mouse	BD Pharmingen	51-1325GR	1/1000	TBST milk	-
p16	mouse	Abcam	Ab54210	1/1000		PBS BSA
GAPDH	mouse	Millipore	mab-374	1/20000	TBST milk	-
TUBULIN	rat	Abcam	Ab6160	1/5000	TBST milk	
ACTIN	goat	Santa Cruz	sc-1616	1/10000	TBST milk	-
p53	mouse	CST	2524	1/1000		PBS BSA
p-ACC	rabbit	CST	3661	1/1000	TBST milk	-
ACC	rabbit	CST	3662	1/1000	TBST milk	-

Table S2. List of antibodies used for western blot analyses. Abbreviations: BSA, Bovine Serum Albumin; CST, Cell Signaling Technologies; IF, Immunofluorescence; PBS, Phosphate Buffer Saline; TBST, Tris Buffer Saline 0.05%Tween; WB, Western Blot.

Duration of SS	ATG5/GAPDH			ATG7/GAPDH			Beclin1/GAPDH		
	HSS	LSS	P value	HSS	LSS	P value	HSS	LSS	P value
2 hrs	1.13±0.03	1.15±0.15	1.00	0.85±0.10	0.94±0.10	0.31	2.19±1.17	1.81±0.46	0.84
6 hrs	1.74±0.33	1.20±0.37	0.13	1.05±0.11	0.86±0.19	0.63	1.57±0.52	1.00±0.17	0.19
12 hrs	1.24±0.19	0.94±0.06	0.31	1.06±0.12	0.94±0.19	0.43	0.94±0.17	1.02±0.11	0.31
24 hrs	1.93±0.53	1.60±0.33	0.30	1.06±0.26	0.73±0.16	0.62	1.07±0.09	1.03±0.07	0.73

Table S3. Shear stress does not modulate ATG5, ATG7 or BECLIN1 expression in HUVECs. Western blot analysis of ATG5, ATG7, BECLIN1. Data are normalized to static condition and expressed as mean ± SEM. n= 5 to 7 per time point and per shear stress condition. There was no significant difference between HSS and LSS in any of these parameters.

	***ApoE*$^{-/-}$*; Atg5*$^{flox/flox}$ (n=9)	***ApoE*$^{-/-}$*; Atg5*$^{flox/flox}$*; VE-cadherin-Cre* (n=11)	***P* value**
Metabolic and morphological features			
Body weight (g)	27.4 (24.3 - 34.8)	28.2 (25.8 - 31.4)	0.76
Male gender (%)	5 (55)	5 (45)	0.44
Arterial blood pressure (mm Hg)	79 (74 - 85)	78 (71 - 83)	0.81
Cholesterol (g/L)	8.9 (7.7 - 10.1)	10.0 (7.5 - 11.3)	0.087
Fasting serum glucose (mg/dL)	84 (77 - 109)	111 (102 - 125)	**0.048**
Spleen weight / body weight (%)	0.5 (0.5 - 0.6)	0.5 (0.4 - 0.6)	0.59
Kidney weight / body weight (%)	ND	ND	-
Liver weight / body weight (%)	4.9 (4.7 - 5.2)	5.0 (4.6 - 5.6)	0.49
Heart weight / body weight (%)	0.6 (0.5 - 0.6)	0.5 (0.5 - 0.6)	0.59
Blood cell count			
WBC (x10^3/mm^3)	4.7 (4.0 – 6.4)	5.4 (3.0 – 9.4)	0.66
Lymphocytes (x10^3/mm^3)	2.9 (2.3 – 3.3)	2.6 (2.1 – 4.4)	0.73
Monocytes (x10^3/mm^3)	0.2 (0.1 - 0.3)	0.2 (0.1 - 0.2)	0.45
Granulocytes (x10^3/mm^3)	2.1 (1.1 – 2.8)	2.7 (0.9 – 3.9)	0.40
RBC (x10^3/mm^3)	6.9 (6.2 - 7.7)	7.3 (6.7 - 7.5)	0.80
Hemoglobin (g/dL)	9.8 (8.5 - 10.4)	10.1 (9.4 - 10.3)	0.66
Platelets (x10^3/mm^3)	626 (556 - 964)	656 (560 - 715)	0.88

Table S4. Metabolic features and blood cell count of 23 weeks old *ApoE*$^{-/-}$*; Atg5*$^{flox/flox}$ *vs. ApoE*$^{-/-}$*; Atg5*$^{flox/flox}$*; VE-cadherin-cre* mice fed a Western diet for 10 weeks. Blood cell count was available for 3 mice per group. Data are expressed as median (interquartile range) or number (%) for the gender. There was no significant difference between both groups in any of these parameters except for fasting glucose (p=0.048).

Abbreviations: ND, not determined; RBC, red blood cell; WBC, white blood cell.

	***Atg5*$^{flox/flox}$** **(n=12)**	***Atg5*$^{flox/flox}$*; VE-cadherin-Cre*** **(n=10)**	***P value***
Metabolic and morphological features			
Body weight (g)	22.4 (20.1 - 27.6)	21.5 (19.9 - 25.0)	0.48
Male gender (number)	5 (42)	4 (40)	0.079
Arterial blood pressure (mm Hg)	78 (73 - 82)	78 (75 - 81)	0.74
Cholesterol (g/L)	1.1 (0.9 - 1.4)	1.4 (1.1 - 1.8)	0.93
Fasting serum glucose (mg/dL)	134 (107 - 144)	125 (108 - 162)	0.93
Spleen weight / body weight (%)	0.4 (0.3 - 0.4)	0.4 (0.3 - 0.4)	0.27
Kidney weight / body weight (%)	0.6 (0.5 - 0.6)	0.6 (0.5 - 0.6)	0.80
Liver weight / body weight (%)	4.0 (3.8 - 4.2)	4.2 (3.5 - 4.5)	0.51
Heart weight / body weight (%)	0.6 (0.5 - 0.7)	0.6 (0.6 - 0.7)	0.91
Blood cell count			
WBC (x10^3/mm^3)	4.3 (3.2 - 5.3)	3.8 (2.7 - 4.8)	0.27
Lymphocytes (x10^3/mm^3)	3.4 (2.8 - 5.0)	3.5 (2.7 - 4.4)	0.89
Monocytes (x10^3/mm^3)	0.3 (0.2 - 0.4)	0.2 (0.2 - 0.3)	0.29
Granulocytes (x10^3/mm^3)	0.2 (0.1 - 0.4)	0.2 (0.1 - 0.2)	0.30
RBC (x10^3/mm^3)	7.1 (6.9 - 7.5)	6.9 (6.5 - 7.6)	0.29
Hemoglobin (g/dL)	13.9 (12.8 - 16.8)	14.3 (12.7 - 15.4)	0.93
Platelets (x10^3/mm^3)	689 (602 - 733)	684 (572 - 787)	0.99

Table S5. Metabolic features and blood cell count of 10 weeks old *Atg5*$^{flox/flox}$ *vs. Atg5*$^{flox/flox}$*; VE-cadherin-Cre* mice fed a chow diet.

Data are expressed as median (interquartile range) or number (%) for the gender. There was no significant difference between the two groups in any of these parameters.

Abbreviations: RBC, red blood cell; WBC, white blood cell.

	***Atg7*$^{flox/flox}$** **(n=12)**	***Atg7*$^{flox/flox}$; *VE-cadherin-Cre*** **(n=10)**	***P value***
Metabolic and morphological features			
Body weight (g)	22.6 (20.2 - 24.1)	21.0 (19.6 - 21.7)	0.27
Male gender (number)	6 (50)	4 (40)	0.46
Arterial blood pressure (mm Hg)	77 (74 - 83)	81 (76 - 84)	0.49
Cholesterol (g/L)	1.5 (1.1 - 1.7)	1.3 (1.1 - 1.6)	0.51
Fasting serum glucose (mg/dL)	150 (139 - 171)	150 (124 - 156)	0.53
Spleen weight / body weight (%)	0.4 (0.3 - 0.5)	0.5 (0.5-0.7)	**0.005**
Kidney weight / body weight (%)	0.6 (0.5 - 0.6)	0.6 (0.6-0.6)	0.55
Liver weight / body weight (%)	5.0 (4.5 - 5.4)	5.1 (5.0-5.3)	0.64
Heart weight / body weight (%)	0.47 (0.45 - 0.49)	0.54 (0.53 - 0.60)	**0.001**
Blood cell count			
WBC (x10^3/mm^3)	3.1 (1.5 - 4.4)	3.3 (2.2 - 3.5)	0.66
Lymphocytes (x10^3/mm^3)	2.8 (1.1 - 3.1)	2.6 (1.8 - 2.7)	0.98
Monocytes (x10^3/mm^3)	0.1 (0.0 - 0.1)	0.1 (0.1 - 0.1)	0.30
Granulocytes (x10^3/mm^3)	0.5 (0.1 - 0.9)	0.6 (0.2 - 1.0)	0.72
RBC (x10^3/mm^3)	6.9 (6.2 - 7.6)	6.1 (5.8 - 6.9)	0.079
Hemoglobin (g/dL)	9.5 (9.1 - 10.6)	9.1 (8.2 - 9.7)	0.18
Platelets (x10^3/mm^3)	657 (456 - 697)	617 (589 - 696)	0.64

Table S6. Metabolic features and blood cell count of 10 weeks old *Atg7*$^{flox/flox}$ *vs.* *Atg7*$^{flox/flox}$*; VE-cadherin-Cre* mice fed a chow diet. Blood cell count was available in *Atg7*$^{flox/flox}$*; and in 9 Atg7*$^{flox/flox}$*; VE-cadherin-Cre mice*.

Data are expressed as median (interquartile range) or number (%) for the gender

Abbreviations: RBC, red blood cell; WBC, white blood cell.

	***Atg5*$^{flox/flox}$** **(n=7)**	***Atg5*$^{flox/flox}$*; VE-cadherin-Cre*** **(n=10)**	***P value***
Metabolic and morphological features			
Body weight (g)	47.1 (43.5 - 52.9)	44.2 (41.8 - 50.7)	0.49
Male gender (%)	7 (100)	10 (100)	-
Cholesterol (g/L)	2.3 (1.8 - 2.9)	3.0 (2.2 - 3.4)	0.19
Fasting serum glucose (mg/dL)	132 (126 - 156)	134 (129 - 144)	0.65
Liver weight / body weight (%)	6.4 (5.1 - 7.1)	4.4 (3.8 - 5.0)	**0.022**
Heart weight / body weight (%)	0.4 (0.4 - 0.5)	0.4 (0.4 - 0.5)	0.47

Table S7. Metabolic features of 64 weeks old *Atg5*$^{flox/flox}$ *vs. Atg5*$^{flox/flox}$*; VE-cadherin-Cre* mice fed a high fat diet for 16 weeks.

Data are expressed as median (interquartile range) or number (%) for the gender.

	***Atg7*$^{flox/flox}$ (n=14)**	***Atg7*$^{flox/flox}$; *VE-cadherin-Cre* (n=10)**	***P value***
Metabolic and morphological features			
Body weight (g)	54.2 (52.4 - 59.6)	54.1 (52.5 - 56.1)	0.69
Male gender (number)	14 (100)	10 (100)	-
Cholesterol (g/L)	2.5 (1.9 - 3.0)	2.0 (1.8 - 2.5)	0.31
Fasting serum glucose (mg/dL)	191 (171 - 207)	184 (159 - 203)	0.66
Liver weight / body weight (%)	5.3 (4.5 - 6.4)	4.8 (3.7 - 6.0)	0.26
Heart weight / body weight (%)	0.3 (0.3 - 0.3)	0.4 (0.3 - 0.4)	**0.028**

Table S8. Metabolic features of 64 weeks old *Atg7*$^{flox/flox}$ *vs. Atg7*$^{flox/flox}$*; VE-cadherin-Cre* mice fed a high fat diet for 16 weeks. Data are expressed as median (interquartile range) or number (%) for the gender.

Figure S1

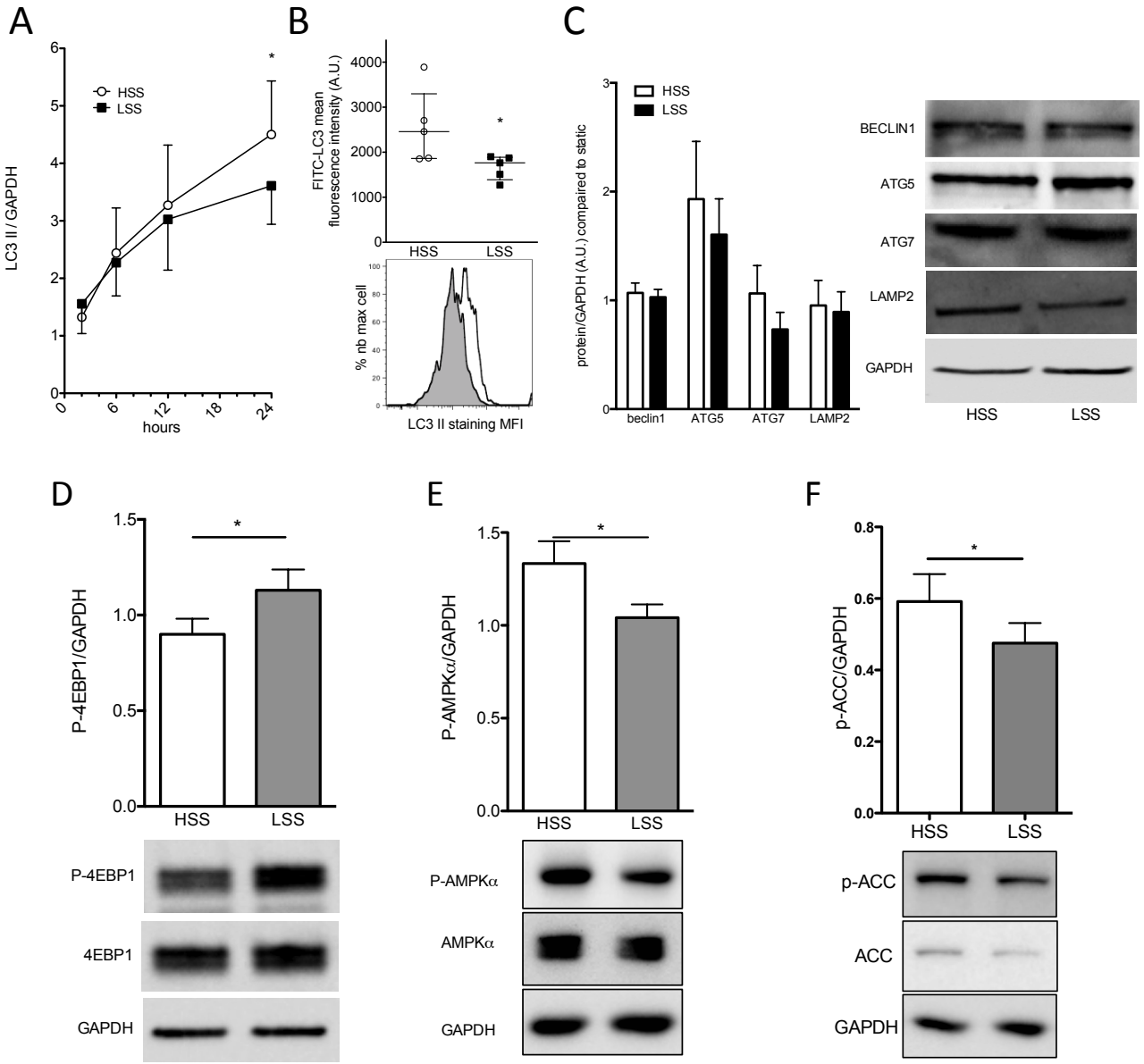

Supplementary Figure 1. Autophagy is defective in endothelial cells exposed to low shear stress. (A) Quantification of LC3 II compared to GAPDH (n ≥ 5 per time point and per condition) in HUVECs exposed to high shear stress (HSS) and low shear stress (LSS). Data are normalized to static condition and are presented as mean ± SEM. (B) Assessment of autophagy level in HUVECs exposed to HSS and LSS for 24 hrs by measuring LC3 staining using flow cytometry (n = 5). Upper panel, quantification; lower panel, representative histogram (gray represents HUVECs exposed to LSS and white HUVECs exposed to HSS). (C) Autophagy related proteins expression in HUVECs exposed for 24 hrs to HSS and LSS (n ≥ 6 per condition). (D-F) 4EBP1, AMPKα and acetyl-CoA carboxylase (ACC) phosphorylations were quantified by western blot in HUVECs exposed to high and low shear stress for 1 (4-EBP1) and 5 min (AMPKα and ACC) (n = 6 for p-4EBP1 and p-AMPKα. n = 9 for p-ACC). *, $p < 0.05$. MFI, mean fluorescent intensity. Figure related to Figures 1 and 3.

Figure S2

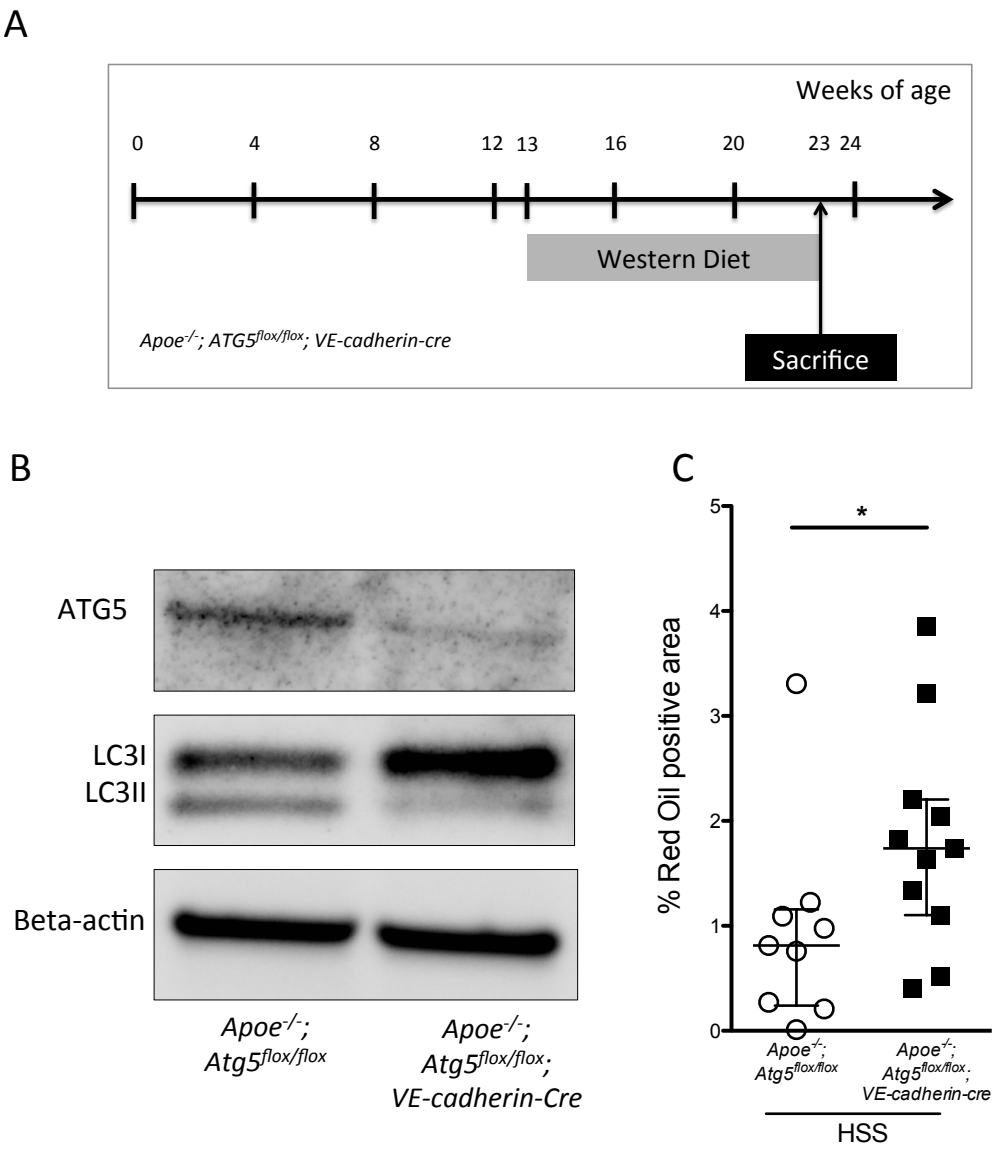

Supplementary Figure 2. *ApoE-/-; Atg5flox/flox; VE-cadherin-Cre* mice are deficient in autophagy in aortic endothelial cells and display increased plaque burden in HSS areas. (A) Protocol to investigate atherosclerosis formation in *Apoe-/-; Atg5flox/flox* and *Apoe-/-; Atg5flox/flox; VE-cadherin-Cre* mice. (B) ATG5 and LC3 levels evaluated by western blot in murine aortic endothelial cells isolated from *Apoe-/-; Atg5flox/flox* and *Apoe-/-; Atg5flox/flox; VE-cadherin-Cre* mice (representative of 2 pools of 4 mice). (C) Quantification of *"en face"* red oil staining of atherosclerotic lesions in the aorta of these mice excluding the ostia of branching points. *, $p < 0.05$. Figure related to Figure 4.

Figure S3

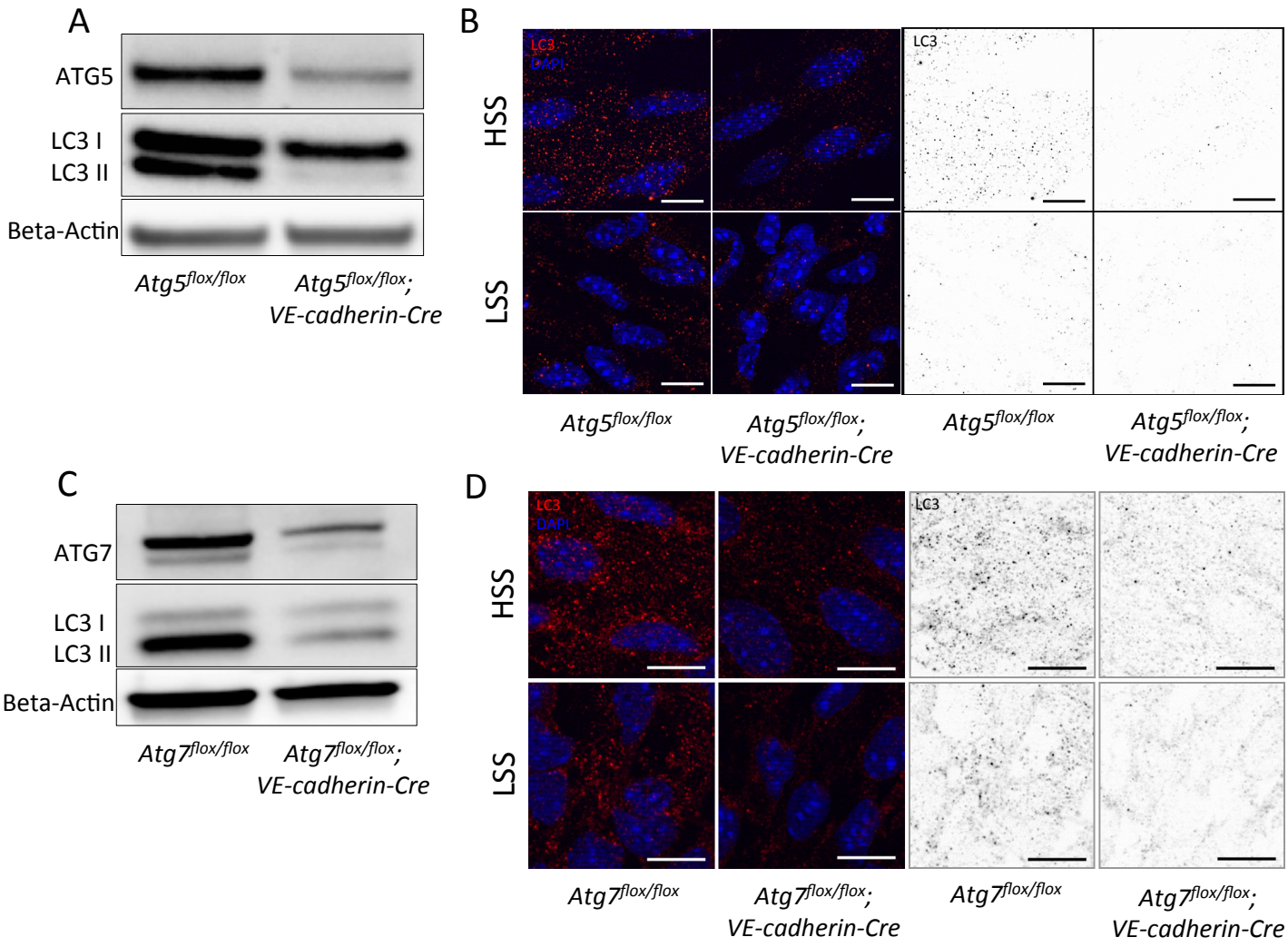

Supplementary Figure 3. *Atg5$^{flox/flox}$; VE-cadherin-Cre and Atg7$^{flox/flox}$; VE-cadherin-Cre* mice are deficient in autophagy in aortic endothelial cells. (A) ATG5 and LC3 levels evaluated by western blot in murine aortic endothelial cells isolated from *Atg5$^{flox/flox}$* and *Atg5$^{flox/flox}$; VE-cadherin-Cre* mice (representative of 2 pools of 4 mice). (B) representative images of LC3 *en face* staining of the aorta of 10 week old *Atg5$^{flox/flox}$ vs. Atg5$^{flox/flox}$; VE-cadherin-Cre* mice (red, LC3; blue, DAPI; n = 5; bar scale, 10 µm; N = 5). (C) ATG7 and LC3 levels evaluated by western blot in murine aortic endothelial cells isolated from *Atg7$^{flox/flox}$* and *Atg7$^{flox/flox}$;VE-cadherin-Cre* mice (representative of 2 pools of 4 mice). (D**)** Representative images of LC3 *en face* staining of the aorta of 10 week old *Atg7$^{flox/flox}$ vs. Atg7$^{flox/flox}$; VE-cadherin-Cre* mice (red, LC3; blue, DAPI; bar scale, 10 µm).-Related to Figure 5.

Figure S4

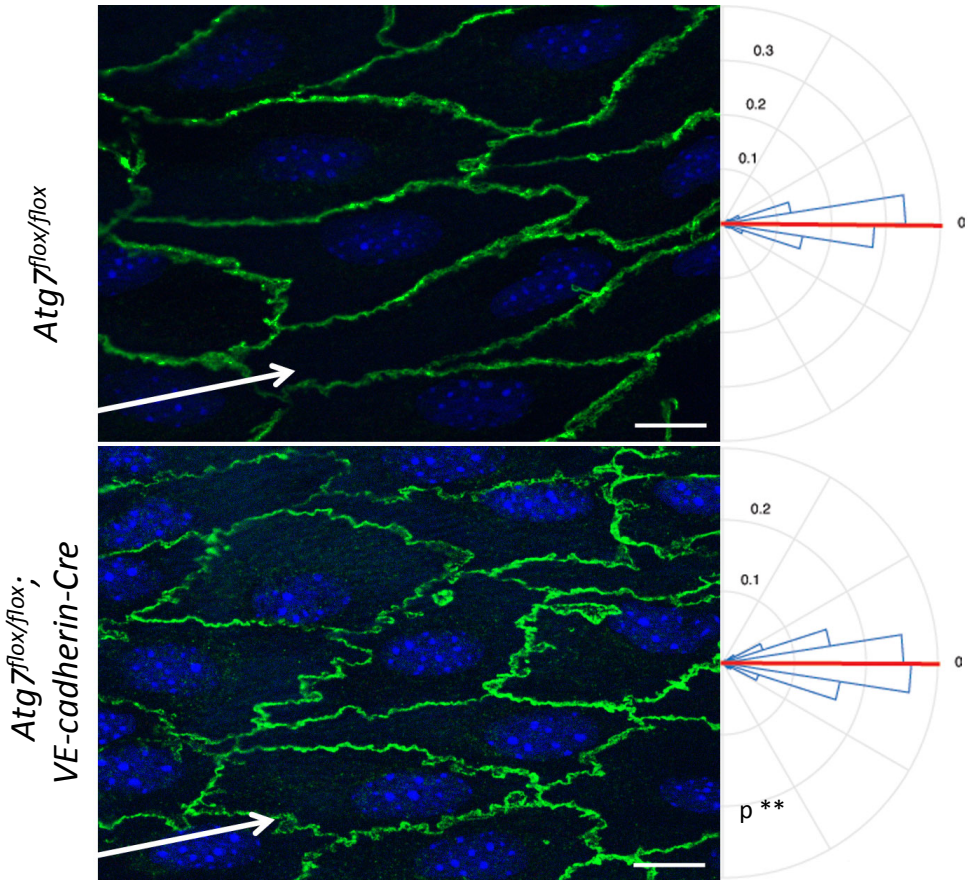

Supplementary Figure 4. Deficiency in endothelial autophagy impairs endothelial cells ability to align in the direction of flow. Quantification of cell alignment in direction of flow in the linear part of the aorta (HSS) of *Atg7*$^{flox/flox}$ or *Atg7*$^{flox/flox}$; *VE-cadherin-Cre* mice (green, CD144 staining; blue, DAPI; n = 5; bar scale 10 μm). **Kp<0.01

figure S5

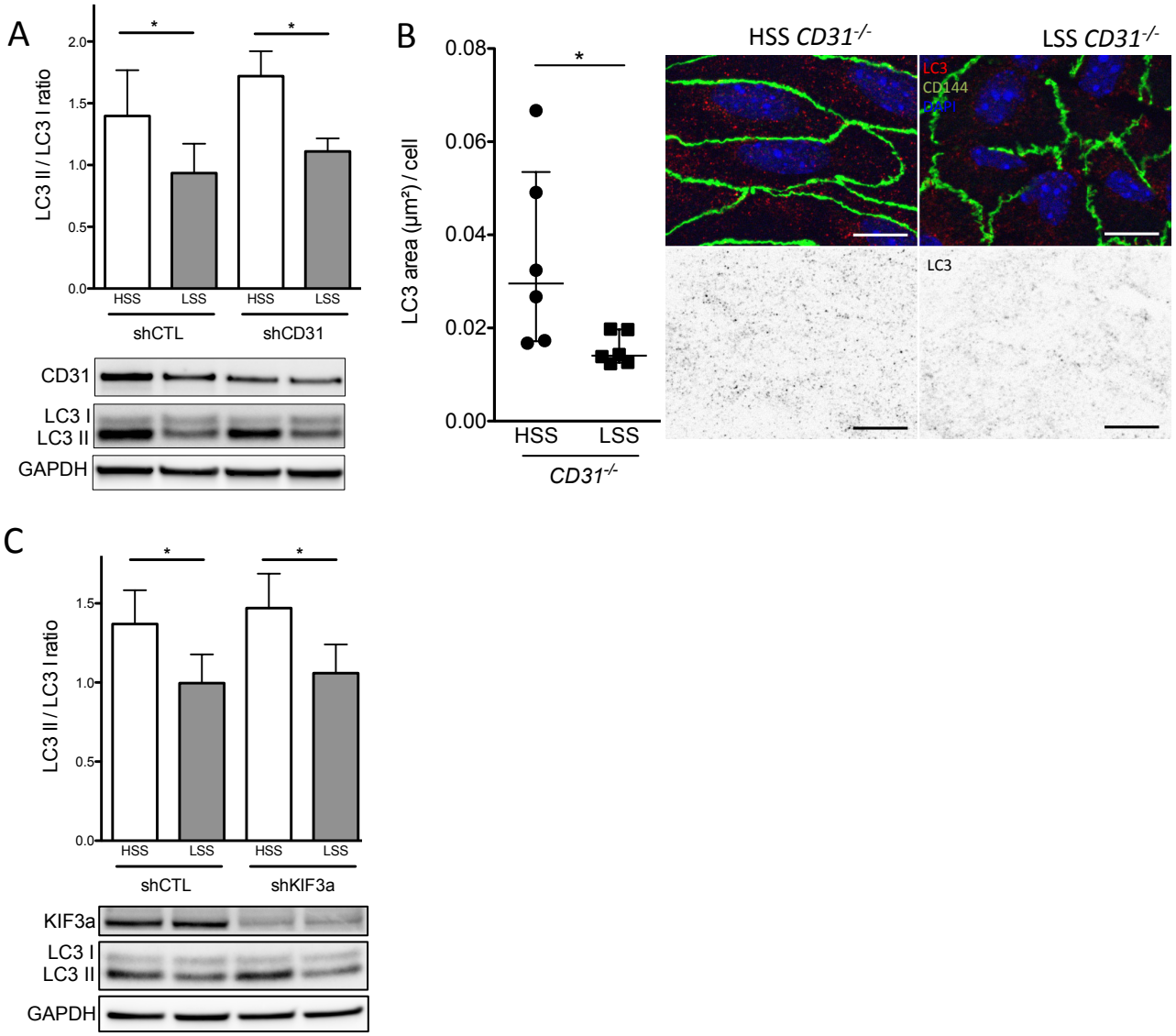

Supplementary Figure 5. The mechanosensor mediating endothelial shear stress effect on autophagy is neither CD31 nor the primary cilium. (A) Western blot analysis of CD31 and LC3 protein expression in HUVECs transduced with a lentivirus expressing CD31 or control shRNA and exposed for 24 hrs to high and low SS (n = 5; shRNA induction: 0.1 mmol/L of IPTG). Data are expressed as mean ± SEM. (B) LC3 *en face* staining of the aorta of 10 week old *CD31-/-* mice (n = 6; green, CD144; red, LC3; blue, DAPI; bar scale, 10 µm). Left, quantification of LC3 area; Data are given as median (horizontal bar) and interquartile range (error bar). Right, representative images. (C) Western blot analysis of KIF3A and LC3 protein expression in HUVECs transduced with a lentivirus expressing KIF3a or control shRNA and exposed for 24 hrs to high and low SS (n = 5, shRNA induction: 1 mmol/L of IPTG). *, $p < 0.05$. HSS, High shear stress; LSS, low shear stress.

Figure S6

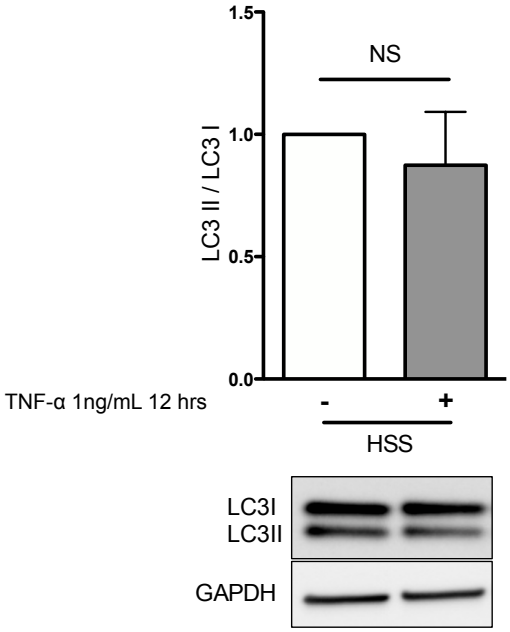

Supplementary Figure 6. TNF-α treatment does not change autophagy level in HUVECs exposed to high shear stress. Western blot analysis of LC3 protein expression in HUVECs exposed for 24 hrs to high SS with or without TNF-α treatment for 12 hrs (n = 6). NS, non significant; HSS, High shear stress.

Figure S7

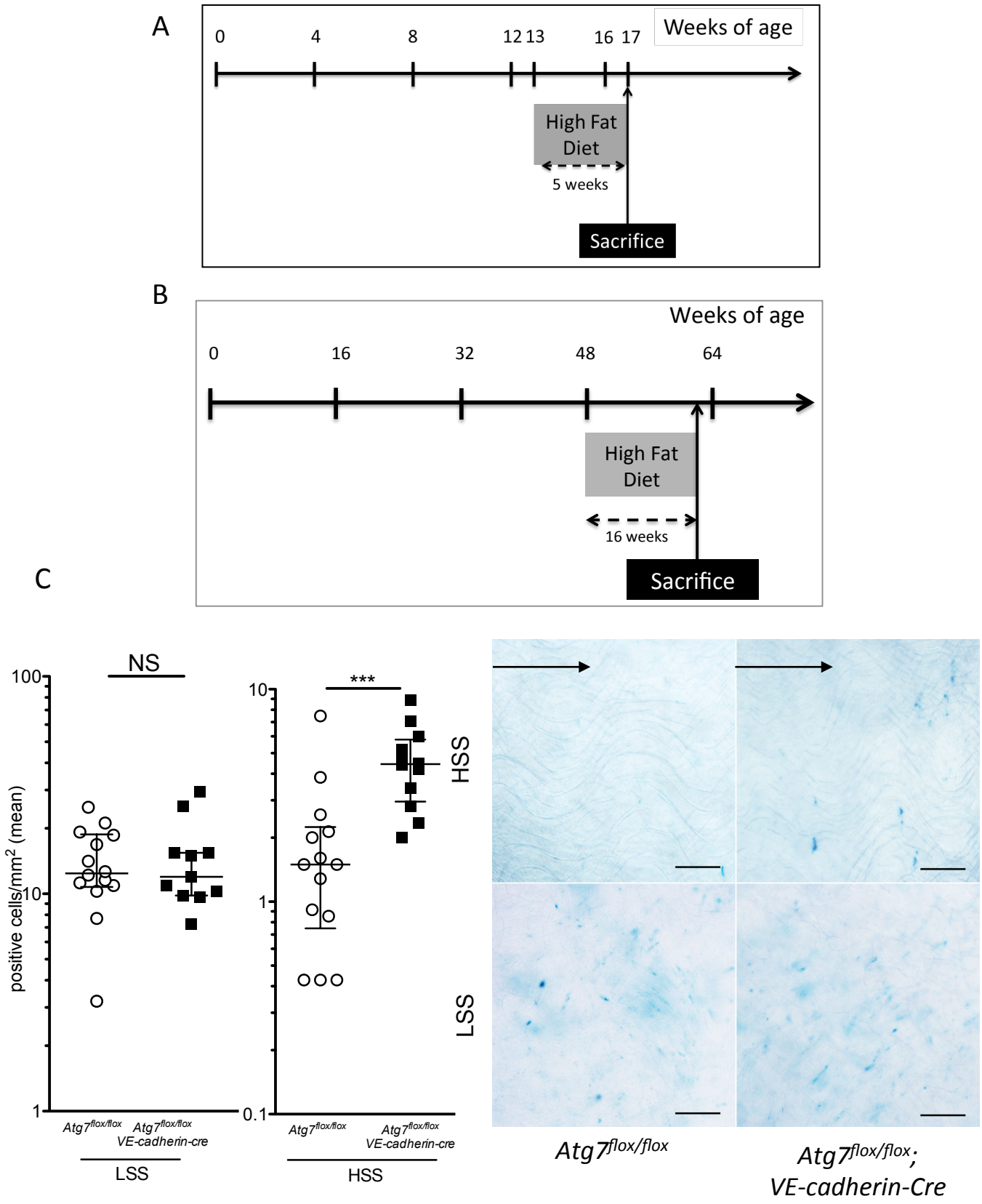

Supplementary Figure 7. Deficiency in endothelial autophagy increases senescence. (A) Protocol to investigate endothelial P53 expression. (B) Protocol to investigate *in vivo* senescence. (C) "*en face*" β-galactosidase staining of the aorta of *Atg7$^{flox/flox}$ vs. Atg7$^{flox/flox}$; VE-cadherin-Cre* mice (n=13 and n=11 respectively). Bar scale, 100 μm; black arrow represents the flow direction. The inner part of the curvature is exposed to SS and the descendant linear part is exposed to high SS. Abbreviations: HSS, High shear stress; LSS, low shear stress. ***, $p < 0.001$ (Mann Whitney test).